Photochemistry and Photobiology, 2010, 86: 1191–1196

Fluorescent-based Solid Sensor for HSO_4^- in Water

Chaoliang Tan, Qianming Wang* and Lijun Ma

School of Chemistry and Environment, South China Normal University, Guangzhou, China

Received 4 June 2010, accepted 2 August 2010, DOI: 10.1111/j.1751-1097.2010.00795.x

ABSTRACT

In this report, we have shown that the encapsulation of the terbium 2-methylimidazole-4,5-dicarboxylic acid complex into inorganic host tetraethoxysilance is considered to be an efficient way for the design of anion sensors. Strong green emission still can be observed when it disperses in pure water. It was found that the luminescence of hybrid material was selectively turned off rapidly (1 s) by hydrogen sulfate compared with the addition of different anions such as F^-, Cl^-, Br^- and I^-. Thin film was successfully prepared and also could be a promising tool for recognizing HSO_4^-.

INTRODUCTION

In the field of chemistry, clinical biology, environmental sciences and biomolecules, ion sensors for the detection of biological process or hazardous chemicals have been extensively studied (1–4). Among many other features, fluorescence was chosen as the most powerful approach to record the chemical recognition event. Therefore, lanthanide complexes have attracted considerable attention as promising sensory materials because of their narrow emission bands and long-luminescence lifetimes, which allow time-resolved measurements to rule out the influence of autofluorescence noise (5–7).

Parker and Gunnlaugsson developed cyclen-based lanthanide complexes for the detection of a group of anions (8–11). Tsukube (12–14) presented that lanthanide tris(β-diketonates) and tripod-lanthanide complexes are available as anion-responsive luminescent compounds. Despite the development of the above research works, there are very limited examples of lanthanide luminescence changes in terms of hydrogen-bonding formation with specific anions (15,16). Furthermore, the prepared lanthanide complexes have relatively lower thermo/photostabilities and are not suitable for the repeated analyses in solutions (17).

Silicate can accommodate a series of photophysically active centers and we focused on the construction of lanthanide-based organic–inorganic hybrid material (18–25). Inspired by the combined merits of both systems, in this work, we introduced a terbium 2-methylimidazole-4,5-dicarboxylic acid complex into an inorganic matrix and developed a novel hybrid material into a solid-sensing material (Fig. 1). As expected, the hybrid material still gives rise to strong green emission in pure water solution. More importantly, the sensing abilities of this material were investigated by addition of various anions, such as HSO_4^-, F^-, Cl^-, Br^- and I^- to water suspension of the assayed bulk material. Highly selective quenching of the hybrid material by hydrogen sulfate anion was observed. According to the spectroscopic analyses, we regard that the quenching process was because of the hydrogen-bonding interaction between the hydrogen sulfate anion and the ligand of the hybrid material. Moreover, thin films were prepared by the same material, which also give rise to luminescence quenching in the presence of hydrogen sulfate anion and could be used as a convenient tool for anion sensing in real-life applications.

MATERIALS AND METHODS

All the starting materials were obtained from commercial suppliers and used as received. ^{1}H-NMR and ^{13}C-NMR spectra were recorded at 293 K using Varian 400 (400 MHz) with TMS as an internal standard. Fluorescence spectra were measured using a Hitachi-2500 spectrophotometer with a 150 W xenon lamp as light source. All the scan speed was fixed at 300 nm min^{-1}. Both excitation and emission slit widths were 2.5 nm. Luminescence lifetime measurements were carried out using an Edinburgh FLS920 spectrometer with a pulse width of 3 μs. LC-MS was measured by Thermo Finnigan LCQ Deca XP Max equipment. Thermogravimetric analysis was carried out using a STA409PC system under air at a rate of 10°C min^{-1}, IR spectra was measured by Fourier transform infrared, and nitrogen adsorption/desorption isotherms were measured at the liquid nitrogen temperature, using an ASAP2020 analyzer. Surface areas were calculated by the Brunauer–Emmett–Teller (BET) method and pore size distributions were evaluated from the desorption branches of the nitrogen isotherms using the Barrett–Joyner–Halenda (BJH) model. X-ray powder diffraction was measured using a Y-2000 X-ray diffractometer of Dandong Aolong Company, China.

For synthesis of 2-methylbenzimidazole, the detailed process was similar to that reported previously (26). A mixture of *o*-phenylenediamine (3.24 g, 0.03 mol) and acetic acid (1.80 g, 0.03 mol) was refluxed for 1 h in HCl (4 M, 35 mL). The green solution was neutralized by ammonia. The white precipitate formed was filtered and recrystallized from water (yield: 3.53 g, 70%).

For preparation of 2-methylimidazole-4,5-dicarboxylic acid (L), the detailed process was similar to that reported previously (26). A solution of chromium trioxide (1.5 g, 0.015 mol) in water (5 mL) was added dropwise to a solution of 2-methylbenzimidazole (2.64 g, 0.02 mol) in glacial acetic acid (15 mL) at 90°C. The reaction mixture was heated at 100°C for a further 5 min and then poured into water (*ca* 200 mL). The precipitate formed was discarded. The filtrate was extracted using chloroform, and the combined extracts were dried (Na_2SO_4) and evaporated. Crystallization of the residue from benzene gives 2-methylimidazole-4,5-dicarboxylic acid [yield: 1.848 g, 70%; ^{1}H-NMR (DMSO-d_6) δ = 2.87 (3H, s, H_a); ^{13}C-NMR (DMSO-d_6) δ = 159.7 (C_a), δ = 146.2 (C_c), δ = 128.2 (C_b), δ = 11.61 (C_d); and MS found: *m/z* 171.7].

The preparation of terbium 2-methylimidazole-4,5-dicarboxylic acid complex was performed as follows (24): 2-Methylimidazole-4,5-dicarboxylic acid (33.8 mg, 0.2 mmol) was dissolved in 8 mL of

*Corresponding author email: qmwang@scnu.edu.cn (Qianming Wang)

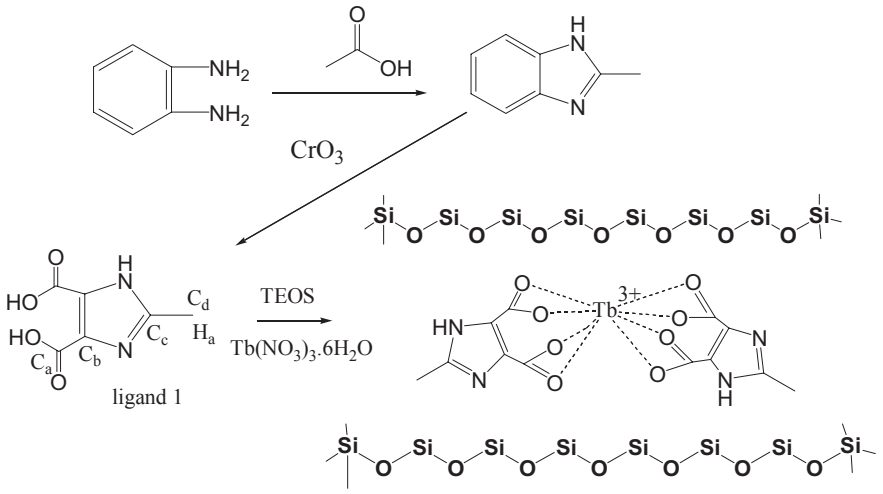

Figure 1. Synthetic process of the hybrid material.

ethanol in a 50 mL round bottom flask, and $Tb(NO_3)_3{\cdot}6H_2O$ (45.3 mg, 0.1 mmol) dissolved in 2 mL ethanol was added to the flask followed by the addition of ammonia (1 mL). The mixture was stirred at 90°C for 1 h. The crude product was washed using ethanol and water, then dried *in vacuo* overnight and the resulting precipitate was collected to give the complex ($TbL_2{\cdot}2H_2O$ (60 mg) as white powder. Elemental analysis found: C, 27.18; H, 2.34; N, 10.59%; Anal. Calcd for $C_{12}H_{12}N_4O_{10}Tb$: C, 27.13; H, 2.28; N, 10.55%.

The preparation of terbium 2-methylimidazole-4,5-dicarboxylic acid containing hybrid material was as follows (24): 2-methylimidazole-4,5-dicarboxylic acid (67.6 mg,0.4 mmol) was dissolved in 5 mL DMSO in a 50 mL beaker, then tetraethoxysilane (TEOS; 416 mg, 2 mmol) and $Tb(NO_3)_3{\cdot}6H_2O$ (90.6 mg, 0.2 mmol) were dissolved in 10 mL water and ammonia (5 mL) was added into the above solution. The mixture was stirred under room temperature for approximately 5 h. Then it was dried at 80°C for 24 h and the resulting precipitate was collected to give the titled complex (300 mg) as white powder.

For preparation of the terbium complex containing TEOS thin films, the detailed process was similar to that reported previously (22). [Tb**L**$_2$] (5 mg) was dissolved in 2 mL of ethanol. This solution was mixed with TEOS (1 mL) and water (1 mL). Two drops of ammonia were then added to the above solution. The mixed solution was stirred at room temperature for 48 h. The glass substrates were cleaned first by rinsing them in distilled water containing a surfactant. As a next step, they were cleaned ultrasonically for 30 min in distilled water containing surfactant, then ultrasonically for 10 min in acetone and finally they were boiled for 10 min in 2-propanol. Finally, the sol-gel solutions were cast on the prepared glass substrates, dried in open air for a week and the thin films were formed.

RESULTS AND DISCUSSION

The IR spectra for ligand **1** (a), Tb**L**$_2$ (b) and the hybrid material containing Tb**L**$_2$ (c) are shown in Fig. 2. The broad bands at 3535 and 3450 cm^{-1} were assigned to be –OH stretching vibrations. Intramolecular hydrogen-bonding formation and molecular packing were detected by the broad band located between 2400 and 2800 cm^{-1}. The intense band at 1917 cm^{-1} is attributed to C=O vibration in COOH groups (19,20). In Fig. 2b, the coordination interactions between the carboxylate and the terbium ion are supported by the bands located at 1575 and 1384 cm^{-1} that is ascribed to the asymmetric (υ_{as}) and symmetric (υ_s) stretching vibrations of carboxylate. In the meantime, the COOH peak at 1917 cm^{-1} vanished completely. The difference between υ_{as} and υ_s is 191 cm^{-1}, showing that the ligand was coordinated with Tb^{3+}

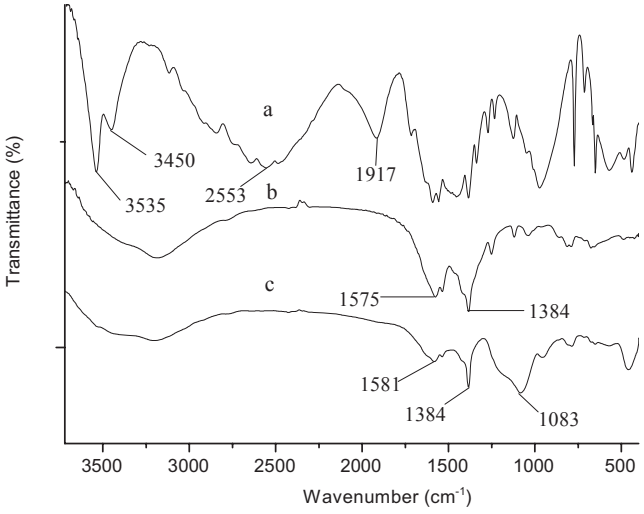

Figure 2. The IR spectra of the ligand (a), terbium complex (b) and hybrid material (c).

through oxygen atoms of carboxyl groups. After incorporation into the silica network, it can be observed that the formation of the silica framework is given by the intense band at 1083 cm^{-1} (Fig. 2c) (21).

^{1}H-NMR spectroscopy was used to study the binding affinity of anions to ligand **1**. Upon addition of 1 equivalent of hydrogen sulfate ion, the H_a protons shifted to downfield (from 2.87 to 3.18 ppm) (Fig. 3), suggesting the binding of ligand **1** to hydrogen sulfate ions in terms of hydrogen interactions to the imidazole-ring NH. Similarly, we also found the shifting of proton to downfield with the addition of 1 equivalent of fluoride ion (Fig. S1; see Supporting Information). We tried analogous NMR experiments of Cl^-, Br^- and I^-, but ligand **1** did not give rise to signal changes in each proton (data not shown).

There are considerable research reports concerning aromatic carboxylic acids and terbium ions because the former have suitable triplet state energy levels for resonant emissive energy of the latter (24,25,27). However, we recently found

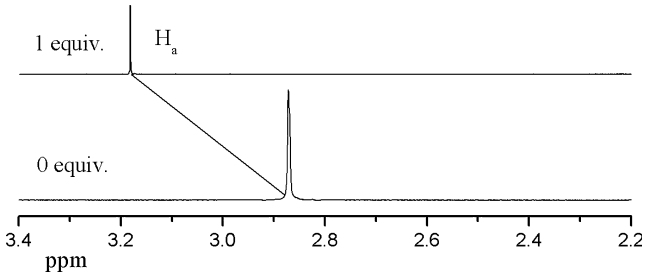

Figure 3. ^{1}H-NMR spectra measured by titration of a DMSO-d_6 solution of pure 1 (1 mM) with 2 equivalents of $[Bu_4N]$ HSO_4.

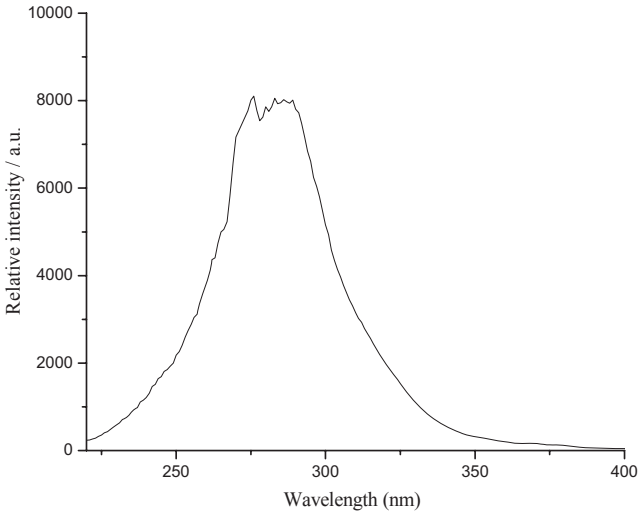

Figure 4. Excitation spectra of the hybrid material powder emission at 545 nm.

that imidazole derivative as a new type of chelating ligands could firmly bind to terbium ions and efficient intramolecular energy transfer occurs. The luminescent binary complex Tb$\mathbf{L}_2$ gave very strong green color emission, but when it was immersed into the water solution, the light was completely quenched by the O–H oscillator of the water. Consequently, to improve the stability of the complex, we incorporated the complex into the inorganic host (TEOS). A more stable hybrid material, which also has a strong green color emission, was fabricated. When emission wavelength was fixed at 545 nm, the excitation spectrum shows a broad band covering from 250 to 310 nm with two peaks at 275 and 290 nm (Fig. 4). Hence, the hybrid is a broad wavelength excitation material. Its emission spectra are shown in Fig. 5. The emission can be interpreted as follows: the excited $^5D_4 \rightarrow {}^7F_J$ transitions exhibit four main components for $J = 6$, 5, 4 and 3, respectively. Under the current situation, no splitting of ^7F_J level could be observed.

As shown in Fig. 6, the hybrid material was dispersed in water with the concentration as low as 10 μg mL^{-1}, which was very efficient in heterogeneous solid–liquid phase. It mainly displayed the characteristic metal-centered emission and could be sensitive to anion interactions. When emission wavelength was fixed at 545 nm, the excitation spectrum shows a sharp peak at 281 nm, which was not very similar to the solid state (Fig. S2; see Supporting Information). After addition of 10^{-5} M hydrogen sulfate anions, green emission from terbium

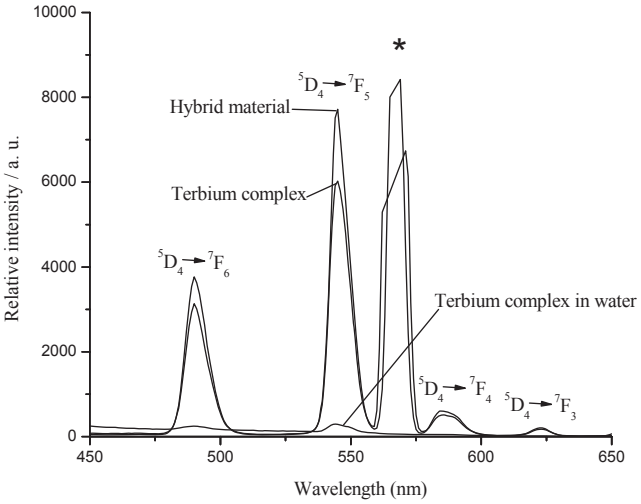

Figure 5. Emission spectra of TbL_2, TbL_2 in water and the hybrid material powder excitation at 282 nm (★: false peak).

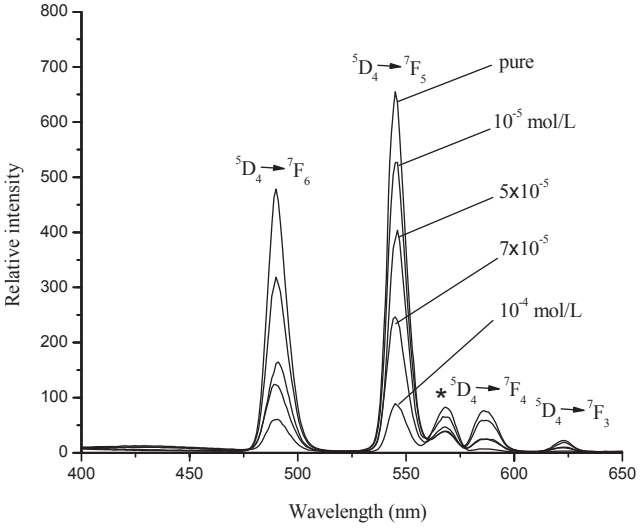

Figure 6. Emission spectra of the hybrid material (10 μg mL^{-1} in water) excited at 281 nm upon addition of 0–10×10^{-5} M of $[Bu_4N]$ HSO_4 (★: false peak).

ions decreased a little. When 5×10^{-5} M hydrogen sulfate anions were added, the characteristic emission of the terbium complex was quenched by 50%. Further quenching was seen in the fluorescence emission spectra upon addition of 7×10^{-5} M of hydrogen sulfate anions. When the concentration of hydrogen sulfate anions increased to 10^{-4} M, the luminescence of the hybrid material was completely shut down. As a consequence, we could observe the sharp and distinguished changes by the naked eye under the excitation of the ultraviolet light (Fig. 7). Continuous addition of the same anion resulted in no change in the luminescence spectra. The above data firmly suggested that this terbium-containing material showed affinity to hydrogen sulfate even in competitive media such as water. Analogous experiments were performed with F^-, Cl^-, Br^-, I^- and $H_2PO_4^-$ (10^{-3} M of corresponding $[Bu_4N]^-$ salts) or within HBF_4 acidic condition (10^{-3} M) (Fig. S3; see Supporting Information). Approximately 10% decrease could

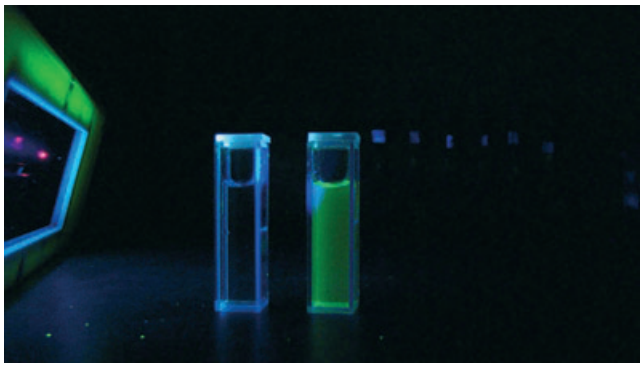

Figure 7. Photograph of hybrid material solution (10 μg mL^{-1} in water) and addition of 10^{-4} M [Bu_4N] HSO_4 (excited by ultraviolet light lamp at 254 nm).

be detected in the emission spectra for halides and HBF_4, indicating that the recognition process has less relationship to acidity in aqueous solution. $H_2PO_4^-$ has led to the largest change (about 20% reduction in intensity), showing that this specific tetrahedral anions might also interact with the receptor. However, we still observed weak green luminescence upon addition of 10^{-3} M anions. Therefore, the emission investigation confirmed that the present hybrid material could be applied as a chemical sensor more suitable for hydrogen sulfate anion.

It is worth mentioning that the fluorescence quenching observed following dipping of powder material into hydrogen sulfate anion solution was found to be almost fully reversible when it was rinsed thoroughly in distilled water. Reusability was evaluated by repeated dipping–rinsing cycles, with the hybrid material fluorescence spectrum being recorded after each step. Typical data are shown in Fig. 8. However, the powder is not very easy to recover for recycling purposes. Subsequently, we coated the hybrid material onto the glass substrate and prepared the thin film for use as a convenient tool as anion sensor. As shown in Fig. S4 (see Supporting Information), the left one is the freshly prepared film. Strong green luminescence can be seen when excited at 254 nm by ultraviolet lamp (the middle one). We can find that it lost the luminescence when it was placed in 10^{-4} M hydrogen sulfate anions solution (the right one). Similar to the powder, the film has no responses in the presence of other anions at the same concentration. Therefore, we can use this film as a tool in real-life applications, such as environmental analysis. The as-prepared films could also be recycled for at least three times. But the responsive time (3–5 h according to the thickness) was longer than the powder material. We thought that the reason might be the as-derived film is too thick. When it was immersed into the aqueous solution, the luminescent complex on the surface was quenched immediately. However, the internal structure was still giving rise to green emission as it needs more time for the anion penetration effect. Thus, we will try to use the spin-coating technique to immobilize the fluorescent probes onto the substrate in the future.

The room-temperature X-ray diffraction pattern from 10° to 70° of the hybrid material is shown in Fig. 9. Broad signals are observed and it could be caused by the existence of a short-range order in the material (28). The broad peak centered on 25° in the XRD pattern of the material was ascribed to be the diffraction signal of the amorphous silica moieties of the

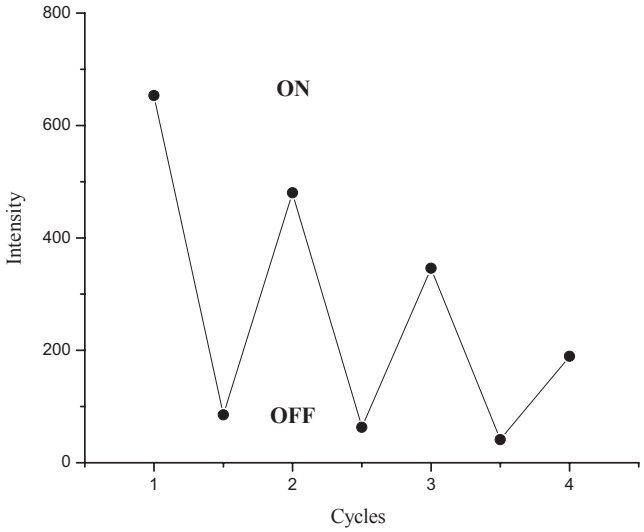

Figure 8. Plot of the fluorescence of the hybrid material with alternated dipping in 10^{-4} M aqueous solution of hydrogen sulfate ions (OFF) and distilled water (ON). The cyclic index is the number of alternating dipping–rinsing cycles, with the vertical axis showing the position of the emission intensity of the hybrid material.

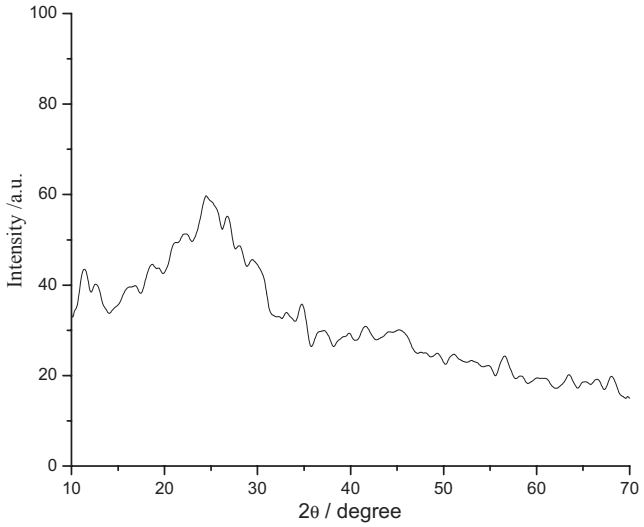

Figure 9. X-ray diffraction patterns of the hybrid material.

hybrid (29,30). In this figure, we cannot observe existence of any types of crystalline patterns such as lanthanide salts, complexes or 2-methylimidazole-4,5-dicarboxylic acid ligand.

Adsorption–desorption isotherms of N_2 were recorded to assess the textural properties of the hybrid material (Fig. S5; see Supporting Information). The specific area and the pore size are calculated by the BET method and BJH model, respectively. It displays a decent surface area (S_{BET}, 100.66 m^2 g^{-1}; pore volume, 0.356 cm^3 g^{-1}; pore diameter, 14.17 nm) without the construction of amphiphilic surfactant templates such as hexadecyl trimethylammonium bromide. The above small pores might be useful as a carrier of particular substances.

Thermal gravimetric analysis provides a reliable way for measuring the thermal stability of the hybrid material. At less than 270°C, which is below the commonly used temperature, terbium complex containing hybrid materials gave a relatively

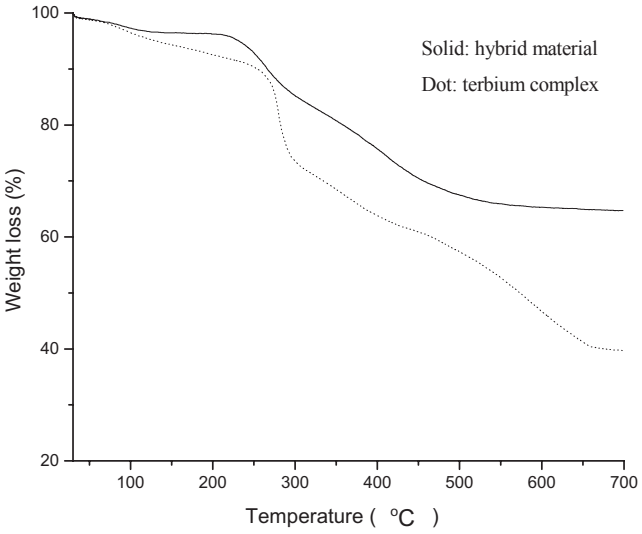

Figure 10. Thermogravimetric analysis traces of terbium complex and hybrid material.

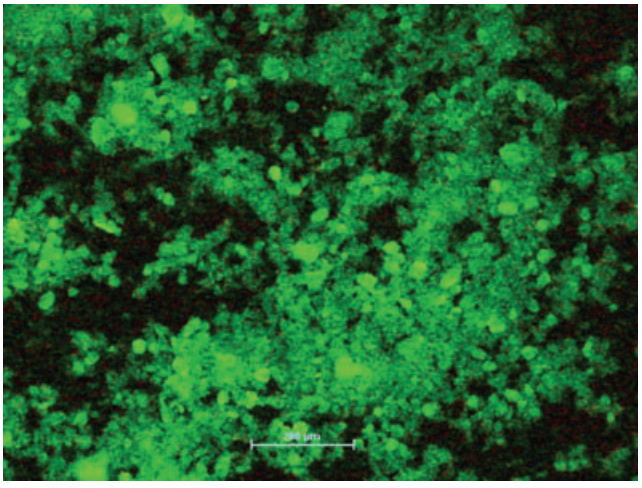

Figure 11. Fluorescence microscope of the hybrid material.

higher thermal stability based on pure complex (Fig. 10). The inorganic host matrix is more stable than the coordination complex, and so when the complex was incorporated into the TEOS, the inorganic host matrix would protect the complex and increase its decomposition temperature.

In addition, fluorescence microscopy was performed to probe the existence of emission species (Fig. 11). The green luminescence image of the figure clearly confirms the localization of terbium complex in TEOS matrices. The lanthanide complex was homogeneously dispersed in hybrid materials and assembled into large aggregates with a diameter of approximately 20–50 μm.

CONCLUSIONS

In summary, we used the lanthanide-based solid sensing material in the heterogeneous solid–liquid phase. Compared with the lanthanide complexes, the material exhibited excellent stability in water when encapsulated into the inorganic host TEOS. It is a breakthrough for lanthanide-based chemical sensor and is possible for practical use. More importantly, upon addition of HSO_4^-, the unique green emission peak of the present terbium complex was significantly quenched through the hydrogen-bonding interaction between ligand **1** and HSO_4^-. However, the addition of excess amounts of F^-, Cl^-, Br^- and I^- showed minor changes of emission bands of terbium ions. This kind of hybrid material can be used several times. In addition, sol-gel film was successfully prepared, which could be directly applied in aqueous solution as a tool for hydrogen sulfate ion recognition. Efforts to apply these results to real-time monitoring and *in situ* detection are currently underway in our laboratory.

Acknowledgements—This work was supported by the National Natural Science Foundation of China (21002035) and Start funding of South China Normal University G21117.

SUPPORTING INFORMATION

Additional Supporting Information may be found in the online version of this article:

Figure S1. ^{1}H-NMR spectra measured by titration of a DMSO-d_6 solution of pure 1 (1mM) with 1 equiv. of $[Bu_4N]$ F.

Figure S2. Excitation spectra of the hybrid material (10 μg/ml in water) emission at 545 nm.

Figure S3. Emission spectra of the hybrid material (10 μg/ml in water) excited at 281 nm upon addition of 10^{-3} mol/L of $[Bu_4N]$ F, Cl, Br, I, H_2PO_4 and HBF_4 acid (*: false peak).

Figure S4. Photograph of thin films (left: room light; middle: UV 254 nm light; right: dipping in 10^{-4} M HSO_4^-). Excited by UV light lamp at 254 nm.

Figure S5. The nitrogen adsorption–desorption isotherms of the hybrid material.

Please note: Wiley-Blackwell are not responsible for the content or functionality of any supporting information supplied by the authors. Any queries (other than missing material) should be directed to the corresponding author for the article.

REFERENCES

1. Robertson, A. and S. Shinkai (2000) Cooperative binding in selective sensors: Catalysts and actuators. *Coord. Chem. Rev.* **205**, 57–199.
2. Kataoka, Y., D. Paul, H. Miyake, S. Shinoda and H. Tsukube (2007) A Cl^- anion-responsive luminescent Eu^{3+} complex with a chiral tripod: Ligand substituent effects on ternary complex stoichiometry and anion sensing selectivity. *Dalton. Trans.* **26**, 2784–2791.
3. Gale, P. A. and R. Quesada (2006) Anion coordination and anion-templated assembly: Highlights from 2002 to 2004. *Coord. Chem. Rev.* **250**, 3219–3244.
4. Anzenbacher, J. P., K. Jursíková and J. L. Sessler (2000) Second generation calixpyrrole anion sensors. *J. Am. Chem. Soc.* **122**, 9350–9351.
5. dosSantos, C. M. G., P. B. Fernández, S. E. Plush, J. P. Leonard and T. Gunnlaugsson (2007) Lanthanide luminescent anion sensing: Evidence of multiple anion recognition through hydrogen bonding and metal ion coordination. *Chem. Commun.* **32**, 3389–3391.
6. Atkinson, P., Y. Bretonniere and D. Parker (2004) Chemoselective signalling of selected phospho-anions using lanthanide luminescence. *Chem. Commun.* **4**, 438–439.

7. Bunzli, J.-C. G. and C. Piguet (2005) Taking advantage of luminescent lanthanide ions. *Chem. Soc. Rev.* **34**, 1048–1077.
8. Parker, D. (2000) Luminescent lanthanide sensors for pH, pO_2 and selected anions. *Coord. Chem. Rev.* **205**, 109–130.
9. Murray, N. S., S. P. Jarvis and T. Gunnlaugsson (2009) Luminescent self-assembly formation on a gold surface observed by reversible "off–on" switching of Eu(III) emission. *Chem. Commun.* **33**, 4959–4961.
10. Gunnlaugsson, T. and J. P. Leonard (2005) Responsive lanthanide luminescent cyclen complexes: From switching/sensing to supramolecular architectures. *Chem. Commun.* **25**, 3114–3131.
11. dos Santos, C. M. G., A. J. Harte, S. J. Quinn and T. Gunnlaugsson (2008) Recent developments in the field of supramolecular lanthanide luminescent sensors and self-assemblies. *Coord. Chem. Rev.* **252**, 2512–2527.
12. Yamada, T., S. Shinoda and H. Tsukube (2002) Anion sensing with luminescent lanthanide complexes of tris(2-pyridylmethyl)amines: Pronounced effects of lanthanide center and ligand chirality on anion selectivity and sensitivity. *Chem. Commun.* **11**, 1218–1219.
13. Mahajan, R. K., I. Kaur, R. Kaur, S. Uchida, A. Onimaru, S. Shinoda and H. Tsukube (2003) Anion receptor functions of lanthanide tris(β-diketonate) complexes: Naked eye detection and ion-selective electrode determination of Cl^- anion. *Chem. Commun.* **17**, 2238–2239.
14. Tsukube, H., A. Onimaru and S. Shinoda (2006) Anion sensing with luminescent tris(β-diketonato)europium(III) complexes and naked-eye detection of fluoride anion. *Bull. Chem. Soc. Jpn* **79**, 725–730.
15. Wang, Q. M. and H. Tamiaki (2009) Highly efficient and selective turn-off quenching of ligand-sensitized luminescence from europium imidazo[4,5-f]-1,10-phenanthroline complex by fluoride ion. *J. Photochem. Photobiol. A.* **206**, 124–128.
16. Gulgas, C. G. and T. M. Reineke (2008) Macrocyclic Eu^{3+} chelates show selective luminescence responses to anions. *Inorg. Chem.* **47**, 1548–1559.
17. Nockemann, P., E. Beurer, K. Driesen, R. V. Deun, K. V. Hecke, L. V. Meervelt and K. Binnemans (2005) Photostability of a highly luminescent europium β-diketonate complex in imidazolium ionic liquids. *Chem. Commun.* **34**, 4354–4356.
18. Binnemans, K. (2009) Lanthanide-based luminescent hybrid materials. *Chem. Rev.* **109**, 4283–4374.
19. Liu, F. Y., L. S. Fu, J. Wang, Q. G. Meng, H. R. Li, J. F. Guo and H. J. Zhang (2003) Luminescent film with terbium-complex-bridged polysilsesquioxanesy. *New J. Chem.* **27**, 233–235.
20. Franville, A.-C., D. Zambon and R. Mahiou (2000) Luminescence behavior of sol-gel-derived hybrid materials resulting from covalent grafting of a chromophore unit to different organically modified alkoxysilanes. *Chem. Mater.* **12**, 428–435.
21. Dong, D. W., S. C. Jiang, Y. F. Men, X. L. Ji and B. Z. Jiang (2000) Nanostructured hybrid organic-inorganic lanthanide complex films produced *in situ* via a sol-gel approach. *Adv. Mater.* **12**, 646–649.
22. Lenaerts, P., A. Storms, J. Mullens, J. D'Haen, C. Görller-Walrand, K. Binnemans and K. Driesen (2005) Thin films of highly luminescent lanthanide complexes covalently linked to an organic-inorganic hybrid material via 2-substituted imidazo[4,5-f]-1,10-phenanthroline groups. *Chem. Mater.* **17**, 5194–5201.
23. Kim, E., H. J. Kim, D. R. Bae, S. J. Lee, E. J. Cho, M. R. Seo, J. S. Kim and J. H. Jung (2008) Selective fluoride sensing using organic–inorganic hybrid nanomaterials containing anthraquinone. *New J. Chem.* **32**, 1003–1007.
24. Wang, Q. M. and B. Yan (2004) Novel luminescent terbium molecular-based hybrids with modified meta-aminobenzoic acid covalently bonded with silica. *J. Mater. Chem.* **14**, 2450–2454.
25. Wang, Q. M. and B. Yan (2005) A novel way to prepare luminescent terbium molecular-scale hybrid materials: Modified heterocyclic ligands covalently bonded with silica. *Cryst. Growth Des.* **5**, 497–503.
26. Baldwin, J. J., P. K. Lumma, F. C. Novello, G. S. Ponticello, J. M. Sprague and D. E. Duggan (1977) 2-Pyridylimidazoles as inhibitors of xanthine oxidase. *J. Med. Chem.* **20**, 1189–1193.
27. Yan, B., H. J. Zhang, S. B. Wang and J. Z. Ni (1998) Intramolecular energy transfer mechanism between ligands in ternary rare earth complexes with aromatic carboxylic acids and 1,10-phenanthroline. *J. Photochem. Photobiol. A* **116**, 209–214.
28. Cerveau, G., R. J. P. Corriu, E. Framery and F. Lerouge (2004) Auto-organization of nanostructured organic–inorganic hybrid xerogels prepared by sol–gel processing: The case of a "twisted" allenic precursor. *Chem. Mater.* **16**, 3794–3799.
29. Carlos, L. D., V. D. Z. Bermudez, R. A. S. Ferreira, L. Marques and M. Assuncao (1999) Sol-gel derived urea cross-linked organically modified silicates. 2. blue-light emission. *Chem. Mater.* **11**, 581–588.
30. Nobre, S. S., P. P. Lima, L. Mafra, R. A. S. Ferreira, R. O. Freire, L. S. Fu, U. Pischel, V. D. Bermudez, O. L. Malta and L. D. Carlos (2007) Energy transfer and emission quantum yields of organic-inorganic hybrids lacking metal activator centers. *J. Phys. Chem. C.* **111**, 3275–3284.